GeroScience
https://doi.org/10.1007/s11357-021-00412-3

ORIGINAL ARTICLE

A quantitative yeast aging proteomics analysis reveals novel aging regulators

Yu Sun · Ruofan Yu · Hao-Bo Guo · Hong Qin · Weiwei Dang

Received: 18 July 2020 / Accepted: 23 June 2021

Abstract Calorie restriction (CR) is the most robust longevity intervention, extending lifespan from yeast to mammals. Numerous conserved pathways regulating aging and mediating CR have been identified; however, the overall proteomic changes during these conditions remain largely unexplored. We compared proteomes between young and replicatively aged yeast cells under normal and CR conditions using the Stable-Isotope Labeling by Amino acids in Cell culture (SILAC) quantitative proteomics and discovered distinct signatures in the aging proteome. We found remarkable proteomic similarities between aged and CR cells, including induction of stress response pathways, providing evidence that CR pathways are engaged in aged cells. These observations also uncovered aberrant changes in mitochondria membrane proteins as well as a proteolytic cellular state in old cells. These proteomics analyses help identify potential genes and pathways that have causal effects on longevity.

Keywords Aging · Calorie restriction · Proteome · Yeast · SILAC

Introduction

A hallmark of aging is the accumulation of deleterious cellular damage, including oxidized, misfolded, and/or aggregated proteins, dysfunctional organelles, and damaged DNA and chromatin structures [11–14]. Various mechanisms exist to remove damaged components in normal young cells and tissues. Enzymes, which include superoxide dismutases (SOD), peroxidases, and peroxiredoxins, remove the ROS generated in the cell [15]. Heat shock proteins direct misfolded and aggregated proteins to either become soluble or degraded by the proteasome [14, 16]. Damaged organelles are disassembled and recycled by lysosomes and autophagy machineries [16, 17]. Exquisite DNA repair and check point systems ensure that DNA damage is fixed prior to replication and transcription [18]. These mechanisms are the basis of the cellular stress

Supplementary Information The online version contains supplementary material available at https://doi.org/10.1007/s11357-021-00412-3.

Yu Sun and Ruofan Yu contributioned equally to the study.

Y. Sun · W. Dang (✉)
Huffington Center On Aging and Department of Molecular and Human Genetics, Baylor College of Medicine, Houston, TX 77030, USA
e-mail: weiwei.dang@bcm.edu

R. Yu
Perelman School of Medicine, University of Pennsylvania, Philadelphia, PA 19104, USA

H.-B. Guo · H. Qin
Department of Computer Science and Engineering, Department of Biology, Geology and Environmental Science, SimCenter, The University of Tennessee At Chattanooga, Chattanooga, TN 37403, USA

Published online: 09 July 2021

response system; enhanced activity through these pathways is often sufficient to enhance longevity, and they are often required for lifespan extension via other genetic and environmental interventions [14]. There are age-dependent changes in these stress response pathways [14, 19], which could be due to their malfunction, leading to aging. However, the underlying mechanisms leading to altered stress response pathways during aging remain elusive.

Aging-related genome-wide gene expression profiling in model organisms points to changes in certain metabolic and stress response pathways, as well as various tissue-specific features [20–24]. Mechanisms of posttranscriptional regulation, such as translation and protein degradation, play an important role in determining cellular proteomes. The lack of correlation between the transcriptome and proteome [25], and the decrease in protein levels for Sir2 and histones in aging yeast [1, 26] warrant a direct analysis of proteomic changes during aging. Among several strategies designed to quantitatively compare proteomes [27], Stable Isotopic Labeling by Amino acid in Cell culture (SILAC) is one of the most reliable quantitative proteomics methods and has been successfully applied in a number of model organisms such as yeast and mice, as well as in human cell culture, and even in patient samples [28]. In a study on the mouse aging proteome, quantitative measurements for over 4000 proteins in brain, heart, and liver tissues from young and old mice were compared and surprisingly few age-dependent changes were found [29], leading to speculation that the mixture of multiple cell types might have obscured the age-related changes and that protein homeostasis would show more dramatic alteration specifically in tissue stem cells of old animals. Since yeast cells have been proposed as a model for adult stem cells [30, 31], studies of the yeast aging proteome could shed light on age-associated proteomic changes in mammalian adult stem cells.

Calorie restriction (CR), or more generally dietary restriction (DR), is the most robust and conserved intervention to extend lifespan in organisms from yeast to primates, suggesting the existence of evolutionarily conserved mechanisms regulating lifespan [32]. Studies in model organisms have suggested the involvement of multiple pathways in mediating longevity and health benefits from DR, including reduced insulin-like growth factor (IGF) signaling [32], elevated sirtuin activity [11], downregulated TOR signaling and ribosome abundance [33, 34], reduced oxidative stress [11], and improved DNA damage repair [35]. For replicative aging of the budding yeast *Saccharomyces cerevisiae*, various CR conditions have been proposed to mediate lifespan extension: enhancing Sir2 function through increased NAD/NADH ratio [36, 37], repressing ribosome biogenesis through downregulation of TOR signaling kinases Tor1 and Sch9 [33, 34], and increasing mitochondria function and oxidative stress response [38–40]. However, exactly how calorie restriction changes the cellular proteome, especially the protein levels for some of the key enzymes regulating these pathways, remains to be explored.

Here, we report a proteomic study for yeast cells during aging under normal and CR conditions and a remarkable similarity between proteomes of aging cells and calorie-restricted young cells, providing evidence that CR pathways are induced in old cells. Our observations also revealed aberrant changes in mitochondria membrane proteins as well as a proteolytic cellular state in old cells. These proteomics analyses can be used to identify potential genes and pathways that have causal effects on aging.

Methods

Strains and media

Yeast strain BY4741 was used for isolation of old cells. All mutant strains for replicative lifespan determination were derived from BY4741 or BY4742. Strain YBJ669, a derivative of BY4742, was used for yeast senescence assay. Strain genotypes are listed in Table S7.

Synthetic complete media (SC, 0.5% ammonium sulfate, 0.17% yeast nitrogen base without amino acids and ammonium sulfate, 0.2% SC mix, and 2% dextrose) containing either regular lysine (Sigma-Aldrich) or ^{13}C-labeled lysine (Cambridge Isotope Laboratories, Lysine 6) were used for SILAC experiments. Standard YPD or SC media without certain amino acids were used in all other experiments. Dextrose (D-glucose) concentrations in all media were either 2% for non-restricted (NR), or 0.5%, or 0.05% for calorie-restricted (CR) conditions as indicated. Methyl methanesulfonate (MMS, Sigma-Aldrich)

was added to SC media as indicated. Standard yeast extract peptone dextrose (YPD) medium (1% yeast extract, 2% peptone, and 2% glucose, with 1.5% agar included for solid medium) was used for all the other yeast experiments.

SILAC labeling

SILAC labeled common reference cells were prepared by continuously culturing BY4741 cells in the SC medium containing ^{13}C-labeled lysine (heavy medium) for about 60 h, a total of about 40 doublings. The culture was maintained within the logarithmic phase by successive dilutions with fresh heavy media in the mornings and evenings. Cells containing unlabeled lysine should have been diluted 10^{12} times; hence, no unlabeled cells should remain in the final SILAC labeled culture. Cells were collected, aliquoted, and stored at − 80 °C. Incorporation of ^{13}C-labeled lysine was verified by mass spectrometry.

Isolation of young and old cells and preparation of whole-cell extracts

Young and old isolation and whole-cell extract preparation were carried out essentially as described previously [1] with the following modifications: SC media containing 2% (NR) or 0.05% (CR) dextrose were used; 3.2×10^9 cells for NR or 2.8×10^9 for CR were labeled by biotin; cell density was always kept within the logarithmic phase in all culturing periods (OD600 < 2.0 for NR and < 0.2 for CR cultures); only old cells from the last (fourth) sort, about 4×10^8 cells, were saved; young cells were collected only from unbound fraction of the first sort; bud scars were stained with WGA Alexa Fluor 488 (Invitrogen); whole-cell extracts were prepared for the saved young and old cell fractions, as well as aliquots of SILAC labeled reference cells, at the same time. Two biological replicate experiments were performed in tandem.

Mass spectrometry

Whole-cell extracts from non-SILAC labeled (light, containing regular lysine) young and old yeast cells grown in either NR or CR medium were mixed in 1:1 ratio with whole-cell extracts from the SILAC labeled (heavy, containing ^{13}C-labeled lysine) common reference cells and loaded on a 4–12% gradient NuPAGE gel (Invitrogen). Approximately 200 µg of protein was loaded per lane. Gel lanes were cut into 18 slices, which were independently further sliced into smaller pieces and then subjected to in gel digestion using the lysC protease (Wako Biochemicals) essentially as described [2]. Briefly, gel slice was dehydrated; 200 µL 10 mM DTT in ammonium bicarbonate was added and then incubated at 50 °C for 45 min. DTT was then removed and 300 µL 50 mM Iodoacetamide in DTT was added to sample, then incubated for 30 min in dark. Iodoacetamide was then removed; sample was washed once with ammonium bicarbonate then twice with acetonitrile. After speedvac to remove all liquids, 100 ng LysC was added to sample for treatment. Extracted proteolytic peptides were desalted using StageTips [3] and then loaded on an EASY-nLC system (Proxeon) connected online to an LTQ-Orbitrap-Velos mass spectrometer (Thermo Scientific). Peptides were separated according to their hydrophobicity using a 5–30% acetonitrile gradient in 2 h on a 25-cm reverse phase column (New Objective) with an inner diameter of 75 µm packed in house with C18 material (Dr. Maisch; Ammerbuch-Entringen, Germany). Five microliters of the sample was loaded in the column. The mobile phase consists of 2 buffers: Buffer A 0.5% HAc (acetic acid) and Buffer B 0.5% HAc and 80% acetonitrile. Flow rate was set at 250 nl/min. This column was maintained at 50 °C in a column oven (Sonation, PRSO-V1) for 140 min. The mass spectrometer was operated in the data-dependent mode to switch between MS and MS/MS. Full-scan MS spectra were acquired with a resolution of 60,000, and for every full scan, the 15 most intense ions were fragmented in the dual-pressure linear ion trap.

Raw data were processed and analyzed using MaxQuant software [4] version 1.1.1.25, where multiplicity was set to 2 for SILAC labeling and digesting enzyme set as LysC; all other parameters were default. The result was then searched with the integrated Andromeda search engine [5] using yeast proteome database UP000002311 from uniprot, against a decoy yeast database. Minimal peptide length was set to 6 amino acids and data was fixed at a maximum false discovery rate of 1% at peptide and protein level; all other parameters were set as

default. Mass spectrometry data were outputted in the form of light/heavy ratios for each detected protein.

Bioinformatics and data analysis

Quantitative proteomic analysis

Ratios of old/young for the NR and CR conditions, as well as the CR/NR ratio for young cells, for each detected protein were calculated from the light/heavy ratios in the mass spectrometry data and transformed to $\log_2$ values. To assess the agreement between biological replicates for each condition, the $\log_2$ values of the ratio between two biological replicates were plotted in scatterplots and the Pearson correlations were calculated. To evaluate the protein level changes, the log2 ratios were averaged between the two biological replicates. Lists of proteins up- or down-regulated for each of the conditions, old/young in NR, CR/NR of young, and old/young in CR, were generated by selecting protein level changes beyond mean ± 1 SD (standard deviation). Benjamini p-value was calculated from log10-transformed light/heavy ratio. Protein information was obtained from the Saccharomyces Genome Database (SGD, http://yeastgenome.org/). All mass-spec data generated in this study is attached in supplementary data 1.

GO analysis and clustering analysis

Clustering analysis was performed with the program Cluster 3.0 (http://bonsai.hgc.jp/~mdehoon/software/cluster/software.htm) using the Euclidean distance as the similarity metric and the complete linkage clustering method. Clustering analysis result was visualized by Java Treeview (http://sourceforge.net/projects/jtreeview/).

Gene ontology (GO) analysis was performed with the DAVID functional annotation tool (http://david.abcc.ncifcrf.gov/) [6, 7]. To reduce redundancy in GO categories, the Functional Annotation Clustering option was used to group similar annotations into clusters. An enrichment score for each cluster was given as a mean of $-\log_{10}$(p-values) of member GO categories with p-values < 0.01.

Fisher's exact test (R statistics software package, http://www.r-project.org/, version 2.12.1) was used to test the null hypothesis that the proportion of proteins in common for two independent observations is less than or equal to random chance.

Even though our aging mass spec datasets include only two biological replicates, comparable to previous studies [50], we have limited statistical power to determine individual differentially regulated proteins. Hence, we only selected proteins with most significant changes for further investigation. However, the main conclusions of our proteomics study, supported by Gene Ontology analysis based on functional categories of cellular proteins, should remain robust.

Protein interaction network (PIN) analysis

The BioGRID [8] protein–protein interaction networks (PIN, only physical interactions are selected) of *S. cerevisiae* (v. 3.5.164) have been used to infer the interacting pairs for which the mean absolute ratio differences are calculated as

$$\Delta Ratio_i = \left| log_2\left(\frac{t_i}{t_0}\right)_{p,A} - \overline{log_2\left(\frac{t_i}{t_0}\right)_{p,B}} \right|, \quad (1)$$

where $\Delta Ratio_i$ is ratio difference of the ith time point t_i ($i = 1 \sim 11$ in eLife15 set and t_i refers to the old cells of present work) compared to the abundance from time point t_0 (or young cells of present work). The mean value was calculated over all interacting pairs (A: B) in the PIN (averaged over 100,580 interactions of the PIN). A total of 10,000 random permutations have been generated from the original PIN, in which the interacting partners have been randomly reshuffled but the degrees of all nodes preserved [9]. The ratio differences of interacting pairs from the permutations were also calculated using Eq. 1 and compared with those from the original PIN.

RNA purification and qPCR

Yeast cells were grown to log-phase and collected and lysed in QIAzol buffer (QIAGEN) by bead beating with 0.5-mm silica beads (Biospec) for 4 cycles (1 min on, 2 min pause on ice). Total RNA extraction was performed by using the miRNeasy Mini Kit (QIAGEN). Reverse transcription was performed using the High-Capacity cDNA Reverse Transcription Kit (Thermo Fisher Scientific) with 1 µg of purified RNA. Quantitative real-time PCR (qPCR) was

performed using the ViiA 7 Real-Time PCR System 475 (Thermo Fisher Scientific). All qPCR primers used are listed in Table S8.

RNA-seq analysis

Total RNA was extracted as described above. Poly-A RNA was purified from 5 µg total RNA with Dynabeads Oligo (dT)25 (Thermo Fisher Scientific). Paired-end RNA libraries were prepared using the NEBNext Ultra Directional RNA Library Prep Kit for Illumina (New England BioLabs). Sequencing of three biological replicates was performed using the Illumina HiSeq 2500 platform. All raw sequencing results are deposited on SRA under bioproject PRJNA715646 and processed RNAseq data attached as Supplementary data 2.

Yeast replicative lifespan assay

Replicative lifespans of yeast strains were determined by using a microfluid platform as described [10] and analyzed by Invitrogen EVOS FL Auto Imaging System. Statistical assessment of lifespan differences was determined using the Wilcoxon rank-sum test in the R statistics software package (http://www.r-project.org/, version 2.12.1).

Yeast protein purification and western blot

Yeast cells were grown to log-phase and collected and lysed in TENG300 buffer (50 mM Tris–HCl, 150 mM NaCl, 1 mM EDTA, 0.5% NP-40, 10% Glycerol) with protease inhibitor. Cells were lysed by bead beating with 0.5-mm silica beads (Biospec) for 6 cycles (1 min on, 2 min pause on ice). Cell lysate was then sonicated by EpiShear™ Multi-Sample Sonicator for 5 cycles (1 min on and 1 min off). The concentration of protein samples was determined by Bradford assay.

For western blot, protein samples were denaturized by mixing with NuPAGE™ LDS Sample Buffer (4X) (Thermo Fisher) and incubated at 70 °C for 10 min. The samples are run on NuPAGE Bis–Tris 4–12% gels with NuPAGE MES SDS Running Buffer (Thermo Fisher). The gel is then transferred to PVDF membrane and blocked by blocking buffer (1% BSA in TBST). The membrane was incubated in primary antibody for 1 h and washed with TBST for 3 times, then incubated in secondary antibody for 1 h before imaging. The membrane was imaged by LI-COR Odyssey imaging system. The antibodies used in this study are listed in Table S9.

Yeast phenotype assay

Yeast vitality assay

An equal number of cells (measured by OD_{600}) from logarithmic phase cultures were washed with PBS, serial-diluted by 10 folds. For glycerol assay, cells were spotted on SC agar media containing indicated dextrose and glycerol.

ATP assay

Yeast cells were cultured in SC media to log phase and measured by BacTiter-Glo™ Microbial Cell Viability Assay kit (Promega). The 96-well opaque-wall plate was read by Synergy™ 2 Multi-Mode Microplate Reader (BioTek).

Mitochondrial membrane potential measurement by flow cytometry assay

Yeast cells were cultured in YPD to log phase and washed by staining buffer (10 mM HEPES with 5% Glucose) for 3 times. Cells were stained with 17.5 nM DiOC6(3) (3,3′-Dihexyloxacarbocyanine Iodide) (Invitrogen D273) for 15 min at room temperature (RT), then washed twice in staining buffer. An equal number of cells for all the experimental groups were measured by CantoII Yellow-Green Carousel (BD Biosciences) and analyzed by BD FACSDiva software and Flowjo software (10.6.0). Another aliquot of cells was treated with 100 µM FCCP (Sigma-Aldrich) for 30 min before measurement as control.

Results

Quantitative proteomic changes in old cells and calorie-restricted cells

Stable-isotope labeling by amino acids in cell culture (SILAC) is an accurate quantitative method to study proteomes in yeast and other systems [25, 41]. We employed SILAC to determine quantitative changes of cellular protein levels in replicatively old cells.

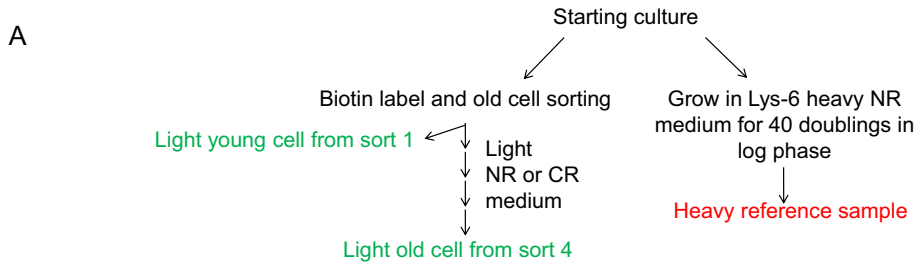

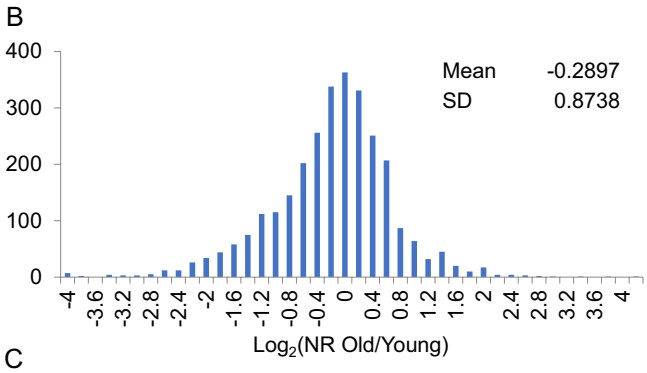

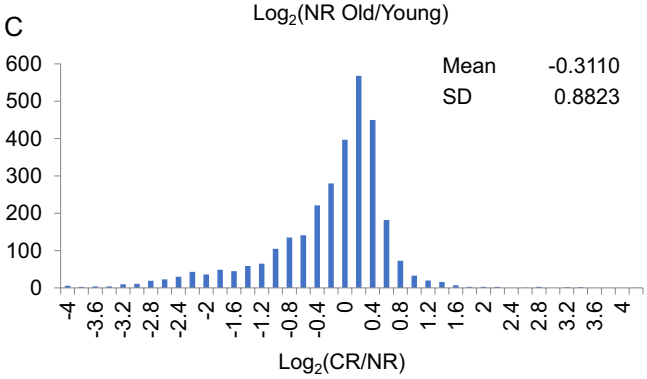

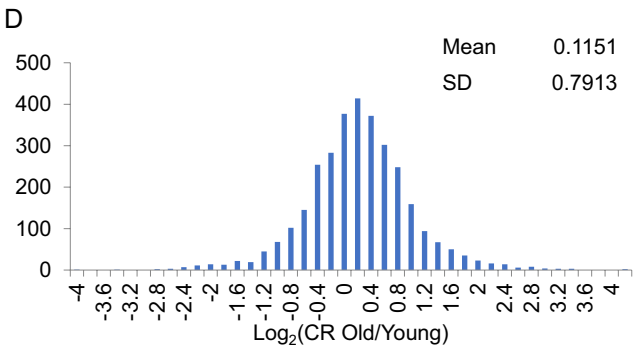

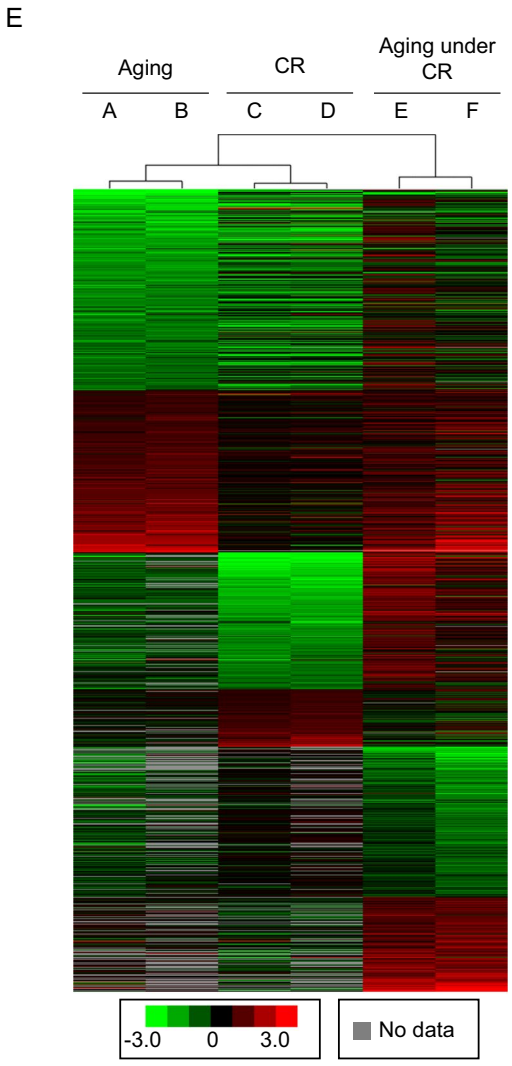

F

	Increase over 2 folds	Decrease over 2 folds	Increase over 4 folds	Decrease over 4 folds
Aging proteome	139	510	15	108
CR proteome	61	469	12	176
Aging proteome under CR	325	206	56	39

◂**Fig. 1** Quantitative proteomic analysis reveals a proteolytic environment in old cells. **a** Experimental procedure of SILAC mass spectrometry measurement. **b–d** Histogram showing the comparison of overall protein fold changes between NR old/young cells (**b**), CR/NR cells (**c**), and CR old/young cells (**d**). An overall reduction shift was both observed in NR old/young group and CR/NR group. **e** Cluster analysis of two biological replicates of all 3 groups shows high similarity between aging and CR cells. **f** The increased and decreased threshold of ± 1SD set for all 3 cell groups

Young and old cells were isolated by biotin surface labeling and purification from cultures prepared with synthetic complete (SC) medium containing 2% glucose (Fig. S1a). A separate culture grown in SC medium containing ^{13}C labeled lysine was used as a common reference. Mass spectrometry (MS) measurements were obtained for equally mixed cell lysates from young cells and the reference, or from old cells and the reference (Fig. 1a), allowing calculation of relative changes during aging. Quantitative measurements for 2845 and 2537 proteins were obtained for two independent aging experiments as biological replicates; 2485 of them were present in both datasets (Fig. S1b); a total of 2897 proteins from both young and old cells were identified and quantified by MS, representing more than half of the measurable proteome [25]. The observed proteomic changes in old cells (ratio of old over young) showed a general consistency between the two biological replicates, with a correlation coefficient of 0.7303 (Fig. S1c). In the combined aging proteomes from both biological replicates, 649 proteins (22.4%) showed changes greater than twofold: 510 were decreased and 139 were increased in old cells (Fig. 1f). A similar shift toward the reduction of most protein levels was also observed when comparing proteins with changes greater than fourfold (Fig. 1f); this is also apparent in the histogram depicting fold changes (Fig. 1b) as well as in the MS intensity-ratio plot (Fig. S1d). The overall shift toward reduced protein levels is consistent with previous observations of reduced protein biosynthesis in aging cells and individuals [42]. Tables S1 to S4 list the top upregulated and downregulated proteins and nuclear proteins. Selected proteins were validated by western blotting using either specific antibodies or epitope tags (Fig. S2).

We compared proteomic changes induced by calorie restriction (CR) in young and old cells grown in SC medium containing 0.05% glucose. Lysates of young and old cells from the CR condition were separately mixed with the same ^{13}C-lysine labeled reference sample described above and analyzed by MS. Similar proteomic coverage was obtained for these two proteomic measurements (Fig. S1e and h) with good to fair correlations between biological replicates (Fig. S1f and i). Interestingly, the CR proteome showed a similar downward trend in protein levels as in the aging proteome, whereas this shift was not observed in the aging proteome under CR (compare Fig. 1 c and b to d, and in Fig. 1f). MS intensity-ratio plots confirmed the quality of MS measurements for these proteomes (Fig. S1d, g, j).

To further examine the similarity among the MS measurements for the aging proteome, CR proteome, and the aging proteome under CR, we performed clustering analysis for all proteins showing level change greater than 1 × standard deviation (SD) in at least one of the MS datasets. As expected, biological replicates closely clustered together (Fig. 1e). Intriguingly, an overall similarity between changes in the aging proteome and the CR proteome emerges in the clustering analysis (Fig. 1e).

Distinct signatures identified in the aging proteome resemble those found in the calorie-restricted proteome

To identify significant pathways or cellular components regulated during aging or calorie restriction, gene ontology analysis was performed for the proteomic data using DAVID [6]. Upregulated and downregulated proteins in the aging proteome, CR proteome, and aging proteome under CR were generated using a 1 × SD threshold (Fig. 2a). We clustered overlapping GO terms in DAVID to extract highly significant GO terms. For each GO cluster, an enrichment score was given (the average negative power of the p values of the GO terms in each cluster), including GO categories with p values less than 10^{-2}. Among the differentially regulated proteins in the aging proteome, distinct functional clusters for upregulated and downregulated proteins were categorized into certain signatures (Fig. 2b and c).

(1) The first signature includes proteins that respond to the low nutrient conditions (blue box). In the upregulated group were various amino acid biosynthetic and metabolic pathways that are nor-

A

	Lower threshold		Upper threshold	
	Log_2	Fold change	Log_2	Fold change
Aging proteome (NR Old/NR Young)	-1.164	2.240	0.584	1.499
CR proteome (CR Young/NR Young)	-1.193	2.287	0.571	1.486
Aging proteome under CR (CR Old/CR Young)	-0.676	1.598	0.906	1.874

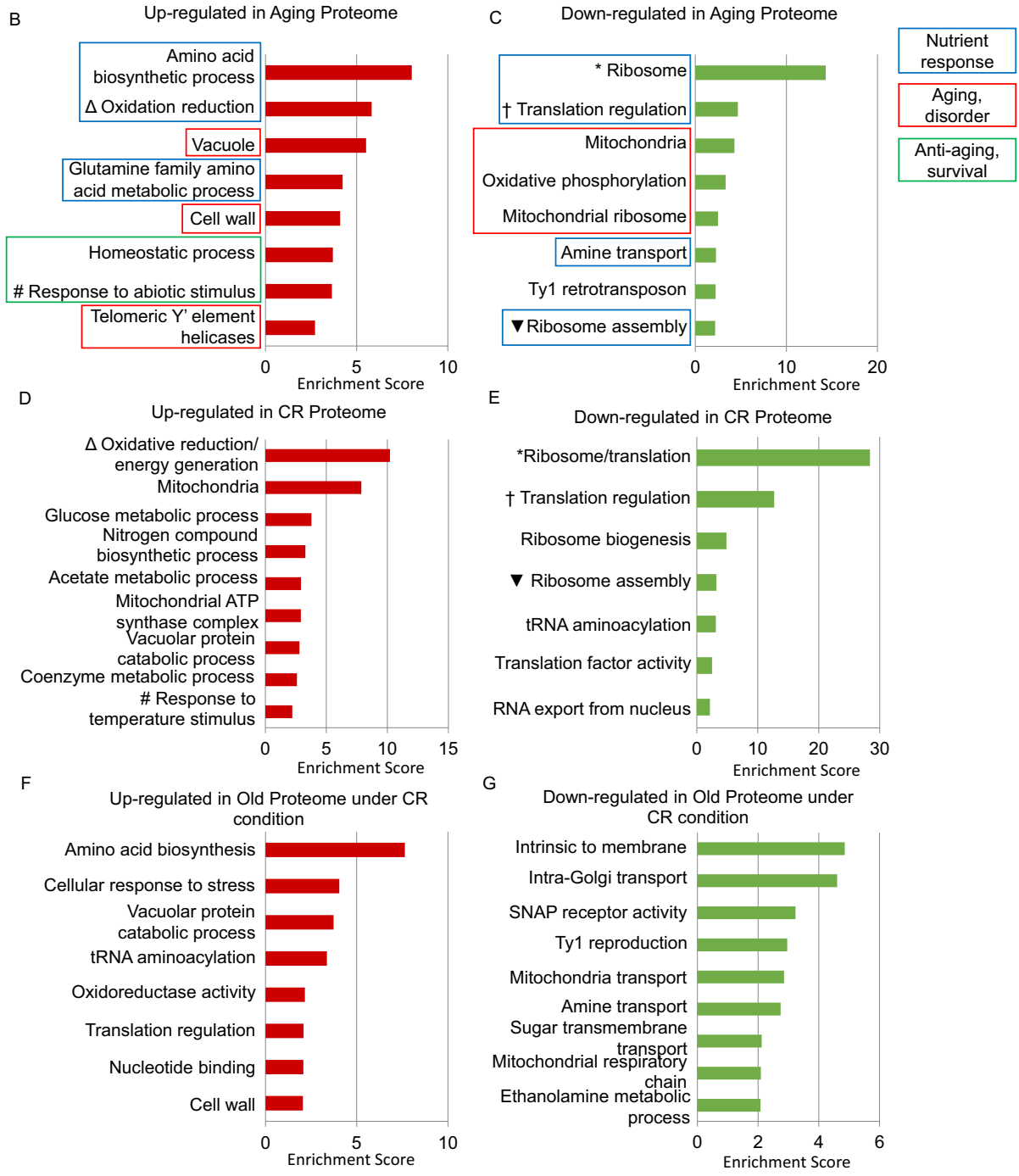

◂**Fig. 2** Gene ontology analysis shows the change of different signature functional groups during aging. **a** The increased and decreased threshold of ± 1SD was set for all 3 cell groups. **b**, **c** Three major signatures of the proteome of aging cells: nutrient response change, aging signs, and protective stress response. Different groups of nutrient response genes are mostly changed. Both up- and downregulated groups have signs of aging disorder, while anti-aging survival genes are upregulated. **d**, **e** The calorie-restricted cells show increased energy generation process and reduced protein biosynthesis, with stress response pathways increased as well. **f**, **g** The old cells under CR condition show a different profile compared to CR/NR, but the stress response is still activated. The symbols Δ, #, *, †, and inverted black triangle represent changes of similar gene groups in aging and CR proteome

mally repressed when cultured in rich media, as well as oxidation/reduction enzymes indicating a shift from fermentation to respiration. In the downregulated group were protein biosynthetic pathways, which are hallmarks of low nutrient availability and starvation. Thus, old cells in rich media shift to a metabolic state that resembles growth in low nutrient conditions. Several nutrient sensing kinases, Tor1 and Sch9, were downregulated in the old cell proteome, consistent with the observed metabolism shift. The upregulation of amino acid biosynthetic pathways may reflect limiting amino acids in old cells, since these pathways are not significantly activated by low glucose (Wang et al., 2010). Indeed, it has been previously shown that limiting non-essential amino acids extends replicative lifespan for yeast (Jiang et al., 2000).

(2) A second signature reveals signs of aging, cellular dysfunction, and disorganization (red box), including increased vacuole and cell wall components, and helicases encoded by telomeric Y' elements, as well as reduced mitochondrial components, oxidative phosphorylation, and mitochondrial ribosomes. Increased cell wall synthesis and its expansion have long been associated with old cells [43]. Reduced mitochondria function and efficiency has also been linked to aging and is attributed to the increased reactive oxygen species (ROS) often observed in old cells [40]. In addition to these GO clusters, all four major histones showed significantly reduced levels in old cells (Fig. 3d) as reported previously [26], suggesting a major dysregulation of transcription and chromatin dynamics.

(3) The third signature is an apparent cellular protective response including upregulation of homeostatic pathways and responses to abiotic stimuli and stress (green box). Yeast cells, similar to higher eukaryotes, accumulate oxidized and damaged proteins and organelles in the cytoplasm and vacuole with age [44, 45], and indeed, the levels of autophagy enzymes were increased. A number of factors contribute to the stress conditions for old cells, including the accumulation of ERCs and damaged proteins, as well as increased levels of ROS and damaged DNA. Thus, the observed upregulation of stress response proteins and enzymes, such as heat shock proteins and DNA damage repair enzymes, would counteract these stresses to promote cell survival.

The proteomic changes in old cells suggested that they are in a state resembling nutrient-limitation. To determine whether these changes were similar with calorie restriction, we examined proteomic changes induced by limiting glucose concentration to 0.05% compared to the normal 2%. We found that the proteome of calorie-restricted cells showed expected downregulated ribosome and protein biosynthetic pathways, as well as upregulated energy generation and carbohydrate metabolic processes (Fig. 2d and e). Interestingly, there was also enrichment in stress response pathways among upregulated proteins under this CR condition (Fig. 2d and Tables S5-6). These similarities confirmed the initial observations (Fig. 1e) that the old cell proteome exhibits evidence of dietary restriction.

We also examined the proteome of old cells cultured in CR conditions and compared them with young CR samples. We found no further significant downregulation of ribosome and protein synthesis or elevation of energy production (Fig. 2f and g). This is potentially because nutrient is not further limited during replicative aging, unlike chronological aging. Interestingly, stress response and vacuolar protein catabolic processes are still significantly upregulated categories in the aging proteome under CR when comparing to young cells grown under CR, suggesting that there are nutrient-dependent and nutrient-independent mechanisms for activating these pathways. Categories similar with the aging proteome, but not found in the CR proteome, such as upregulated cell wall and downregulated mitochondria and Ty1

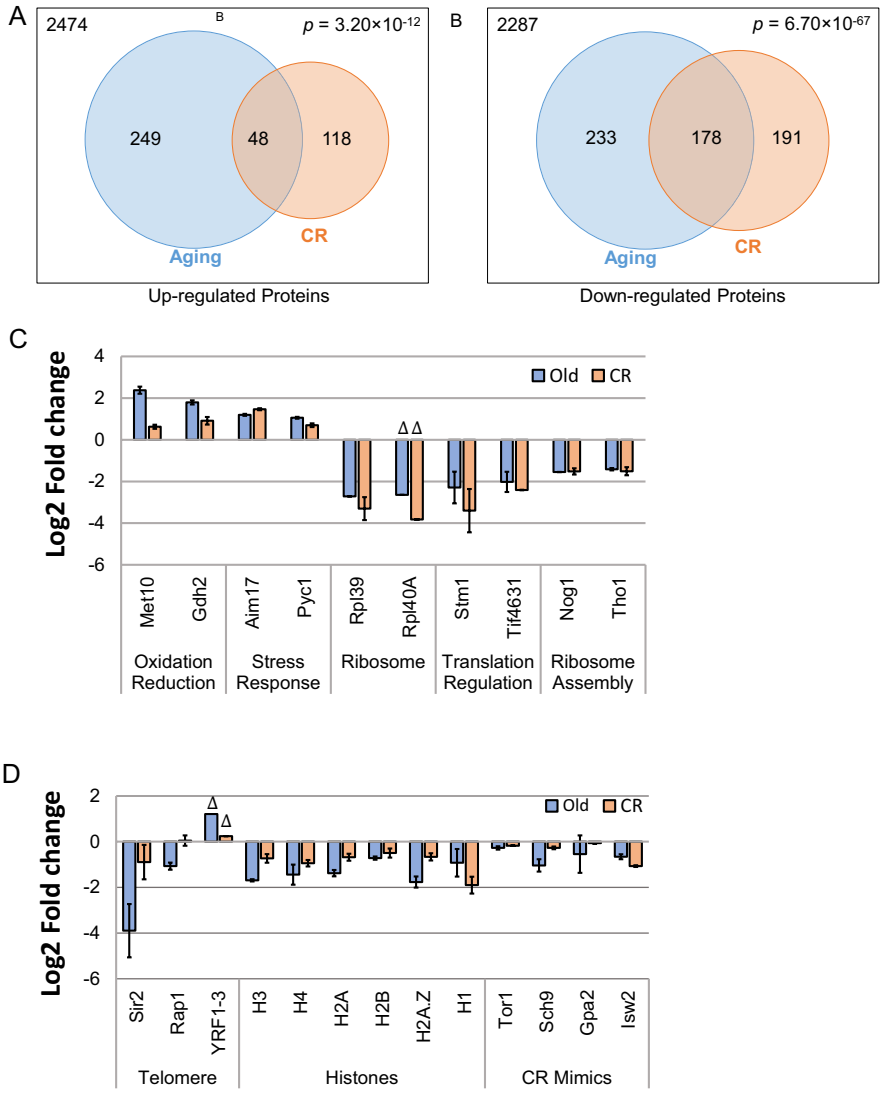

Fig. 3 The proteome of aging cells and calorie-restricted cells show significant similarity. **a**, **b** Venn diagram showing statistically significantly overlapping between proteins upregulated and downregulated, respectively, under normal aging and caloric restriction. **c**, **d** Comparison of protein fold change between CR and old cells, of most enriched/depleted protein in each depicted GO category. Error bars represent SEM; Δ, lack of error bar due to limited detection in mass spec experiments

retrotransposition, likely represent cellular dysfunction and deterioration during aging.

To investigate the similarities in the GO categories between the aging proteome and the CR proteome, we tested the statistical extent of overlap, indicated as pairs of symbols in Fig. 2b–e. We found upregulated stress response and energy generation, as well as downregulated ribosome and protein biosynthesis as common pathways between aging cells and CR cells. Overall, statistically significant overlaps meeting the 1 × SD threshold exist for both up- and downregulated proteins (Fig. 3a and b), further indicating the similarity between these two cellular states. For individual comparisons, the two most significantly changed proteins in each of the similar GO categories show comparable changes in protein abundance (Fig. 3c).

Since upregulation of stress response pathways and inhibition of protein synthesis promote longevity [40, 46], our observation that these protein changes occur in old cells and CR cells, leads to a proposal that old cells intrinsically activate certain CR mechanisms to antagonize aging. Indeed, the observed downregulation of Sch9 and Tor1 nutrient sensing kinases, as well as the downregulated G-protein receptor subunit Gpa2, may trigger activation of CR pathways to benefit old cells (Fig. 3d).

We also noted interesting proteomic changes for several other categories of proteins when comparing

the aging and CR proteomes, including downregulation of an important telomere structural protein (Rap1) in old cells, increased levels of helicases coded by telomeric Y' elements, and downregulation of Sir2 (Fig. 3d), which are consistent with disruption of chromatin structure and the silencing state near telomeres in old cells [1]. As mentioned above, the major histones are reduced in old cells, consistent with previous observations [1, 26], and there were changes in histone H2A.Z levels and the linker histone H1 (Fig. 3d). Importantly, these changes are unlikely caused by increased proportion of arrested cells because quiescent cells arrested due to exhaustion of nutrients do not show reduced histone levels [47].

Variations of the abundance of interacting proteins become less synchronized during aging

Loss of protein homeostasis, or proteostasis, is one of the prime hallmarks of aging [48]. Deficiency of the proteostasis network underlies many aging-related disorders [49], and a recent proteome and RNA-sequencing study showed the degeneration of protein stoichiometry during aging [50]. Using the data set by Janssens et al. [50] (eLife15 set) at 12 different time points across yeast lifespan (from 7.8 to 72.3 h) and our own data detected at both normal YPD (NR) and calorie-restricted (CR) conditions, we calculated the fold changes of all genes between old cells and young cells. For the eLife15 set, the abundance at $t_0 = 7.8$ h is used as reference (or young cells), and those at t_i ($i = 1$ to 11) are treated as old cells. We then compared such ratio change between all interacting pairs collected in the BioGRID (v. 3.5.164, physical interactions) protein–protein interaction network (PIN) [8]. The arrows indicate the mean absolute ratio differences at different t_i ($i = 1$ to 11, data from different time are shown in different colors, see color bars in Fig. S3a). At both protein and mRNA levels in Elife15 dataset, the ratio differences gradually expand during aging, with the ratio differences at older age (i.e., at $t_{11} = 72.3$ h) being most significant. In comparison, our data (Dang seq) showed an even larger increase of the ratio differences at both the protein and mRNA levels (Fig. S3b) than eLife15 set. In addition, our results also indicate that CR could reverse the expansion of mentioned ratio differences, especially at mRNA levels. The differences observed between the eLife15 set and our data (Dang set) (Fig. S3c) could be explained because different genes were chosen for analysis or different experimental conditions. Moreover, we observed that for the eLife15 set, at earlier time point of the lifespan (e.g., $t_1 = 10.7$, $t_2 = 14$), the ratio difference is not significantly different than those calculated from the random permutations. However, at older age (e.g., $t_{11} = 72.3$, and also in the Dang set at both NR and CR conditions), the ratio differences from the original PIN became significantly smaller than random permutations ($p < 1 \times 10^{-5}$, as for 10 k random models). Therefore, our results suggest that the aging process eventually enlarges the abundance differences (ratios) of interacting proteins, and that this enlargement is significantly smaller than random expectations in cells with older ages or under CR conditions.

Npc2 is an aging factor that regulates mitochondrial metabolism through ergosterol distribution

One application of the proteomic analysis is to predict the causal factors of aging. The proteins that decrease with age are usually considered beneficial factors for longevity, while the proteins that increase with age can be either cause or consequence of aging. We picked the top-changed proteins from different experiment groups and GO categories and tested their replicative lifespan (Fig. 4a). DNA replication regulation pathway and unfolded protein response pathway are longevity-promoting pathways. The proteins that are mostly downregulated in these two pathways showed significantly shorter lifespan when deleted. Proteins controlling protein homeostasis showed mixed results for lifespan regulation. Among these proteins we found out two targets that can significantly increase lifespan when deleted: *NPC2* and *FET5*.

Yeast Npc2 is a sterol transport protein. It is the homolog of mammalian Niemann-Pick disease protein NPC2 [51]. Niemann-Pick disease is caused by mutations in either *NPC1* or *NPC2* genes [52]. The homologs of mammalian NPC1 and NPC2 in yeast are *NCR1* and *NPC2* [51, 53]. Ncr1 is a vacuolar membrane protein that regulates sphingolipid distribution and metabolism [54]. Yeast Npc2 binds to Ncr1 to facilitate the integration of sterol into vacuolar membrane [55]. Using microfluid-based measurement, we found that deletion of either *NCR1* or *NPC2* can significantly extend yeast replicative lifespan in a

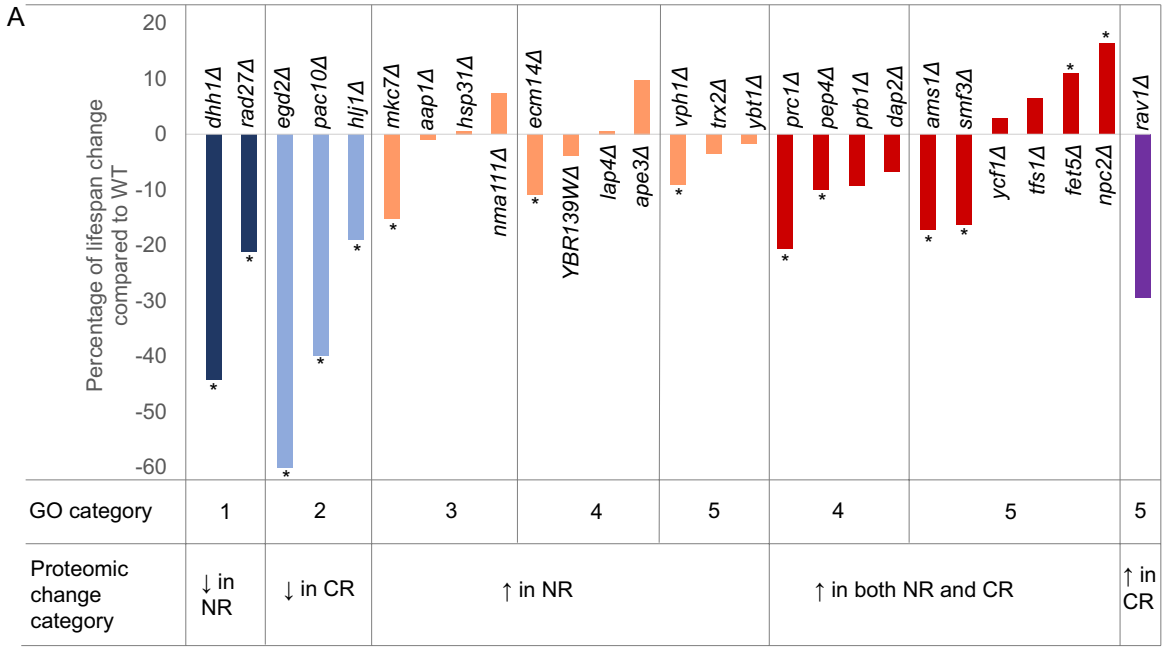

GO legend: 1. DNA replication 2. Unfolded protein binding 3. Peptidase activity 4. Vacuolar peptidase activity 5. Vacuolar protein

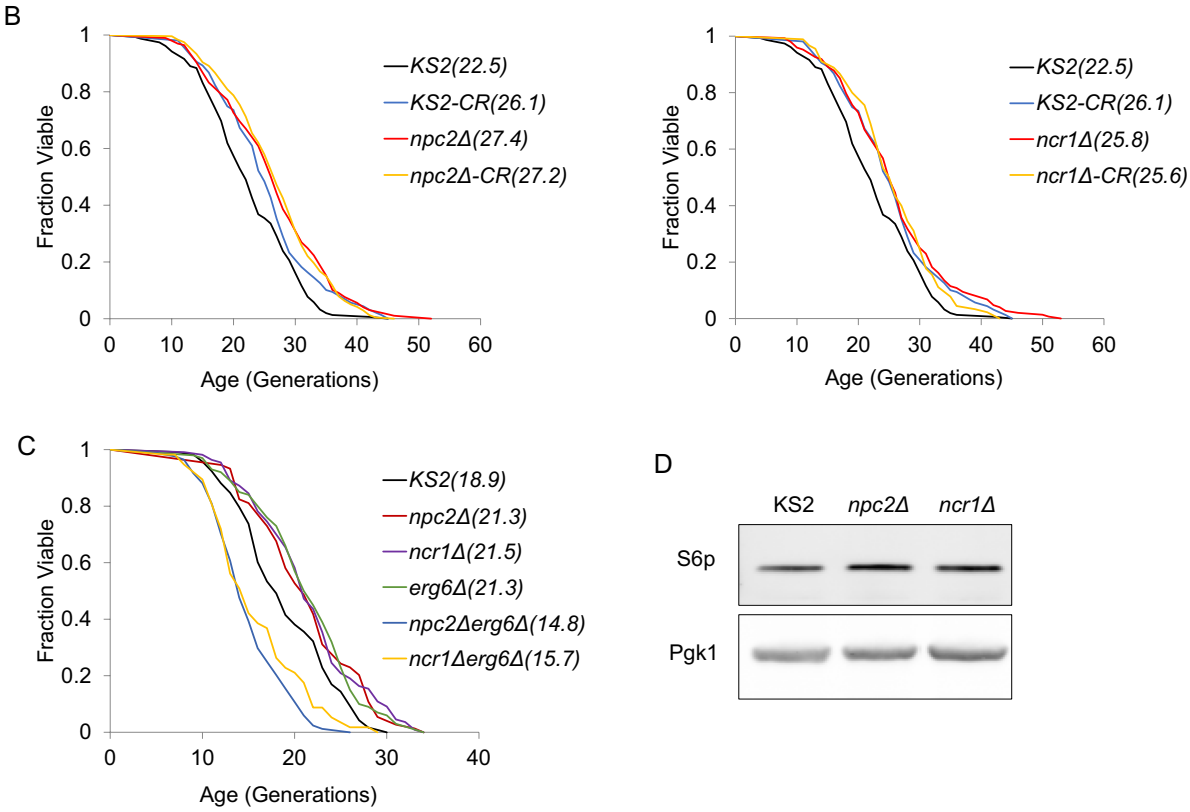

◀ **Fig. 4** The proteomic analysis is a tool for the screening of aging factors. **a** Lifespan analysis of top up- and downregulated proteins shown in their GO categories and experimental groups. (p-value: $dhh1\Delta = 1.35 \times 10^{-14}$, $rad27\Delta = 0.000143$, $egd2\Delta = 3.11 \times 10^{-21}$, $pac10\Delta = 2.92 \times 10^{-11}$, $hlj1\Delta = 0.002037$, $mkc7\Delta = 0.002962$, $ecm14\Delta = 0.000389$, $prc1\Delta = 1.89 \times 10^{-5}$, $pep4\Delta = 0.002345$, $ams1\Delta = 3.66 \times 10^{-7}$, $smf3\Delta = 0.004507$, $fet5\Delta = 0.029053$, $npc2\Delta = 0.000624$, $vph1\Delta = 0.039323$, $rav1\Delta = 2.82 \times 10^{-9}$, for all strains $N > 70$). **b** CR cannot further extend the lifespan of *npc2Δ* (**a**) and *ncr1Δ* (**b**) cells. (p-value compared to KS2: $npc2\Delta = 0.000052$, KS2-CR = 0.005966, $npc2\Delta$-CR $= 4.37 \times 10^{-7}$, $ncr1\Delta = 0.002315$, $ncr1\Delta$-CR = 0.002176, for all strains $N > 100$). Note that the lifespan of WT cells is shorter in microfluidic experiments (~20) because the system captures a mixture of young and old mother cell. **c** Deletion of ERG6 extends lifespan, while *npc2Δerg6Δ* and *ncr1Δerg6Δ* strains have significantly shorter lifespan. (p-value compared to KS2: $erg6\Delta = 0.001572$, $npc2\Delta erg6\Delta = 4.76 \times 10^{-8}$, $ncr1\Delta erg6\Delta = 0.000145$, for all strains $N > 70$). **d** Western blot of S6p shows that S6p level is similar between WT and *npc2Δ* cells

CR-dependent manner (Fig. 4b). Consistent with the fact that Npc2 is upregulated in both aging and CR proteome (Fig. 4a), this result shows that deletion of *NPC2* possibly activates CR-like mechanism to antagonize aging.

Since both Npc2 and Ncr1 are involved in cellular lipid distribution and metabolism, we tested if ergosterol, the yeast cholesterol, plays a role in lifespan regulation. Erg6 is a component of ergosterol biosynthesis pathway [56]. Deletion of Erg6 also significantly extends lifespan (Fig. 4c). However, double deletion of either *NCR1* or *NPC2* together with *ERG6* shortened lifespan (Fig. 4c). These data indicate that a balance of ergosterol in the cell is necessary for lifespan maintenance and disruption of ergosterol transport is beneficial for longevity.

To further explore the mechanism of NPC2-mediated longevity pathway, we performed transcriptome analysis of WT and *npc2Δ* cells. GO analysis showed that mitochondrial genes were the most downregulated category in *npc2Δ* cells, most of which are involved in oxidative phosphorylation process (Fig. 5a). This result implicates impaired mitochondrial function in *npc2Δ* cells. To find out the downstream mitochondrial targets of the *NPC2*-regulated pathway, we tested several downregulated mitochondrial genes in the *npc2Δ* transcriptome, including *MEF1* and *MSN4*. Mef1 is mitochondria translation elongation factor [57], responsible for biosynthesis of several necessary components of mitochondrial electron transport chain [58]. Msn4 is a transcription factor that triggers stress response. It has been shown that Msn4 works together with Msn2 to activate sirtuins and promote longevity under TOR regulation [59]. Lifespan epistasis showed that Mef1 was necessary for *npc2Δ*-mediated lifespan elongation, while MSN4 is dispensable (Fig. 5c). This result suggests OXPHOS function is required for *npc2Δ*-mediated longevity effect.

Since many mitochondrial genes are downregulated, we next tested the functional readout of mitochondria in *npc2Δ* cells to see if mitochondrial function is critical for the Npc2-mediated longevity pathway. We first performed a carbon source survival test. *npc2Δ* cells survive better on non-fermentable carbon source compared to WT (Fig. 5b), indicating the *npc2Δ* cells have improved non-fermentation respiration when glycolysis is disabled. In conclusion, deletion of *NPC2* could benefit lifespan through alteration of mitochondria activity.

Several mitochondrial pathways regulate yeast aging [60]. Cox1 is subunit I of cytochrome C oxidase and is often used as an indicator of mitochondrial genome and their copy number. Quantitative PCR of *COX1* showed slightly but not significantly reduced mitochondrial DNA copy number in *npc2Δ* cells (Fig. S4a). This result is consistent with downregulation of Mef1 in *npc2Δ* cells, which is needed for *COX1* translation. Deficiency in mt-DNA or OXPHOS respiration can trigger retrograde signaling to activate nuclear downstream targets [61]. Cit2 is a well-defined downstream target of retrograde activators Rtg1 and Rtg3, while Cit1 is another reader [62]. We tested the expression of *CIT1* and *CIT2* by qPCR and found no significant difference between WT and *npc2Δ* cells (Fig. S4b and S4c). rho0 cells, which lack mitochondrial genome, are used as positive control. In summary, mitochondrial copy number was slightly reduced in *npc2Δ* cells, but retrograde signaling was not triggered. We then tested mitochondrial ATP production and mitochondrial membrane potential. ATP level is decreased in *npc2Δ* cells in both YPD and glycerol culture (Fig. 5e). *npc2Δ* cells produced less ATP than WT in not only YPD but also glycerol, where ATP is only produced by OXPHOS, implicating an impaired oxidative phosphorylation apparatus. When cultured in YPD media, the reduced ATP production in *npc2Δ* cells is possibly due to reduced MT copy number or impaired respiratory chain. However,

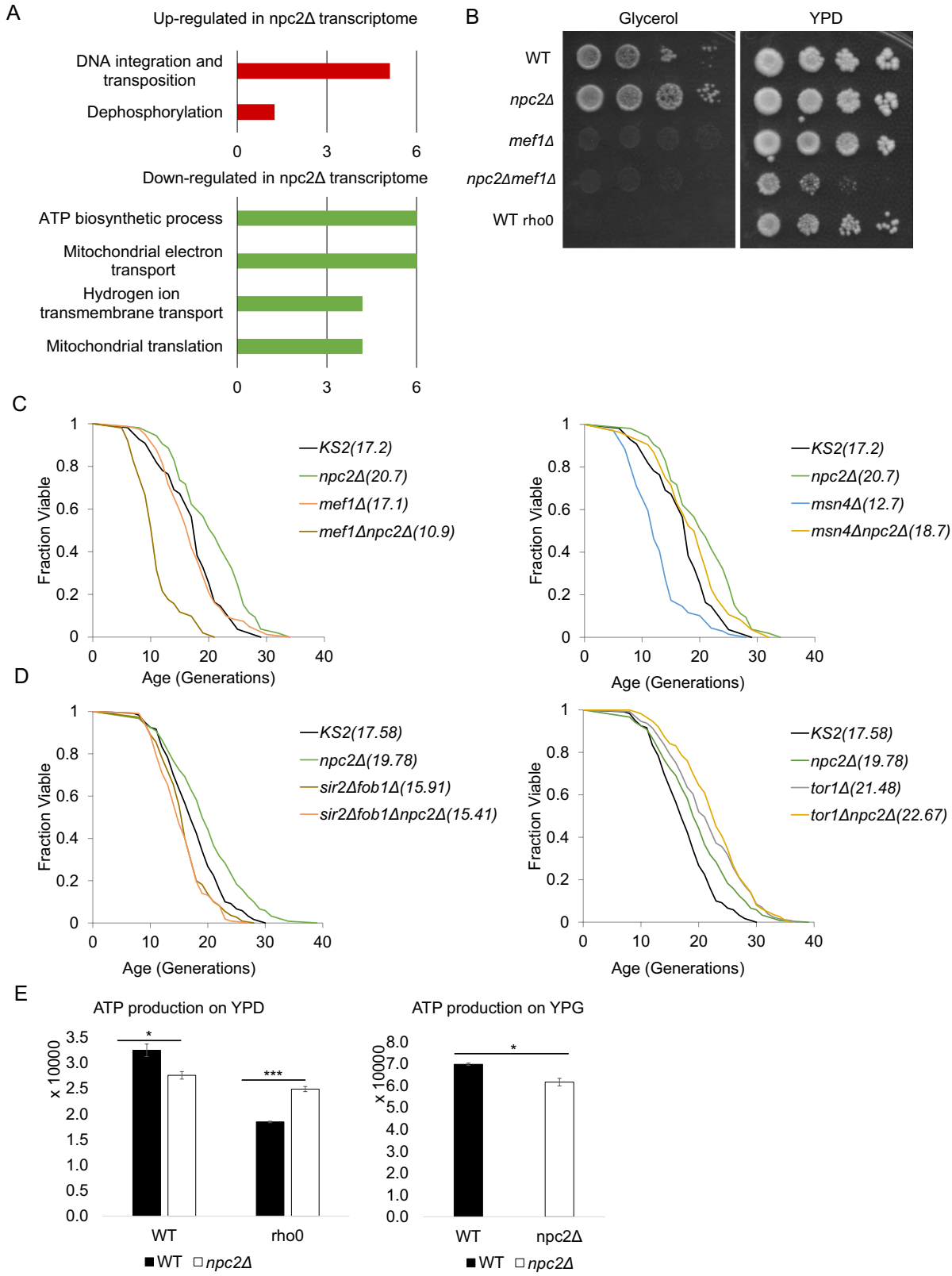
A
Up-regulated in npc2Δ transcriptome
DNA integration and transposition
Dephosphorylation
0
3
6
Down-regulated in npc2Δ transcriptome
ATP biosynthetic process
Mitochondrial electron transport
Hydrogen ion transmembrane transport
Mitochondrial translation
0
3
6
B
Glycerol
YPD
WT
npc2Δ
mef1Δ
npc2Δmef1Δ
WT rho0
C
Fraction Viable
Age (Generations)
KS2(17.2)
npc2Δ(20.7)
mef1Δ(17.1)
mef1Δnpc2Δ(10.9)
KS2(17.2)
npc2Δ(20.7)
msn4Δ(12.7)
msn4Δnpc2Δ(18.7)
D
Fraction Viable
Age (Generations)
KS2(17.58)
npc2Δ(19.78)
sir2Δfob1Δ(15.91)
sir2Δfob1Δnpc2Δ(15.41)
KS2(17.58)
npc2Δ(19.78)
tor1Δ(21.48)
tor1Δnpc2Δ(22.67)
E
ATP production on YPD
x 10000
WT
rho0
WT
npc2Δ
ATP production on YPG
x 10000
WT
npc2Δ

◂ **Fig. 5** NPC2 regulates lifespan through mitochondria and Sir2-mediated pathway. **a** Transcriptome analysis result shown in GO categories. Mitochondrial genes are the most downregulated category. **b** *npc2Δ* cells show better growth under glycerol anaerobic test. Rho0 cells are used as control. **c** Epistasis analysis of *NPC2* and *MEF1* shows epistatic effect on lifespan (left), while *NPC2* and *MSN4* do not (right). (p-value: *mef1Δ* & *mef1Δ npc2Δ* $= 4.53 \times 10^{-11}$, *msn4Δ* & *msn4Δ npc2Δ* $= 7.97 \times 10^{-10}$, for all strains N > 70). **d** Epistasis analysis of NPC2 and SIR2FOB1 shows epistatic effect on lifespan, while NPC2 and TOR1 do not. **e** ATP production test shows reduced ATP production in *npc2Δ* cells in both YPD (left) and YPG (YP + Glycerol) (right) medium. (p-value: YPD-WT& *npc2Δ* = 0.026124, YPD-rho0-WT& *npc2Δ* = 0.000243, YPG-WT& *npc2Δ* = 0.01059, N = 3)

when electron transport chain in impaired in *rho0* condition, *npc2Δ* cells still produce more ATP than WT, suggesting stronger glycolysis activity.

Mitochondrial membrane potential is determined by proton pumps and is a way to measure cellular oxidative phosphorylation function [63]. Flow cytometry of DiOC6, which measures mitochondrial membrane potential, showed no significant difference between WT and *npc2Δ* cells (Fig. S4d). In *rho0* cells, *npc2Δ* showed increased mitochondrial membrane potential, consistent with its higher ATP production (Fig. 5e). Taken together, we conclude that in the long-lived *npc2Δ* cells, the overall mitochondrial oxidative function is inhibited, whereas glycolysis activity is increased, hence a metabolic shift toward glycolysis.

Discussion

Using the yeast replicative aging as a model, our results provided a comprehensive unbiased proteomic study of aging cells; our findings demonstrate distinct signatures of the aging proteome and revealed the partial proteomic resemblance between the aging and CR proteomes. These novel findings led to the hypothesis that old cells exploit mechanisms of CR to antagonize aging. By analysis of the aging proteome, and cross-examination of multiple high throughput data and genetic approaches, we demonstrate a novel longevity mechanism activated by calorie restriction. Inhibition of the chromatin remodeling ATPase Isw2, through reduced protein levels in old cells, or reduced cellular energy states in CR condition, derepresses a cohort of stress response genes, especially the DNA damage repair pathway utilizing homologous recombination. This finding represents the first evidence for the role of chromatin remodeling ATPases in aging regulation.

By testing the lifespan of the top-changed proteins from the aging proteome, we identified several potential aging factors, further validating the confidence of the proteomic screen. Among them, *NPC2*-mediated longevity pathway is a vacuole-to-nucleus pathway that involves sterol metabolism, which has never been reported before. As the homolog of *NPC2* in human is a known disease-causing gene, finding out its role in aging would be very helpful to elucidate its pathological mechanism in higher eukaryotes. The working model is summarized in Fig. S4e.

Shared signatures between older cells and calorie-restricted cells

Plentiful evidence exists to associate aging with profound changes in protein synthesis, modifications, and turnover [42]. Most aging proteomic studies to date examined age-related proteomic changes in specific animal tissues. Although these studies provided some insights to link aging with profound metabolic changes, most of the results were highlighted by tissue-specific features [64, 65]. Another study of various aging mouse tissues by SILAC found few functional clues from bulk tissue samples representing multiple cell types [29]. Thus, these previous results suggest that there is complexity and heterogeneity of age-related proteomic changes in the cell.

Yeast, as a single-cell eukaryotic organism, provides an excellent tool to allow proteomic studies at both the cellular and organismal level, and yet avoiding the complexity of tissue-specific effects, as well as the problem with heterogeneous cell types found in animal tissues. Such a simple model system allows for discovery of general functional alterations during aging.

In this study, we used the yeast replicative aging model system and examined quantitative proteomic changes featured in old cells and calorie-restricted cells, as well as age-associated changes when cells were cultured under the CR condition. Quantitative measurements were obtained for more than half of the measurable yeast proteome, an unprecedented proteomic coverage for an aging study. Functional analysis revealed distinct signatures representing features of metabolic response, aging and dysfunction,

as well as anti-aging and survival. In addition, we observed proteomic changes previously reported, such as downregulation of Sir2 and histone proteins. Proteomic changes in several categories in the aging proteome resemble those found in cells grown under calorie-restricted conditions, including downregulated ribosome abundance, assembly, and protein translation, and upregulated metabolic pathways and stress response pathways. This observation led us to the hypothesis that old cells exploit CR mechanisms to antagonize aging. Indeed, the enzymes involved in CR-repressed pathways, such as Tor1, Sch9, Gpa2, and Isw2, were all downregulated in old cells (Fig. 3c, S2). The mechanism leading to downregulation in old cells of these negative longevity regulators remains to be explored. They could involve an altered protein homeostasis state in old cells, such as elevated autophagy pathways and vacuolar proteolytic enzymes. Alternatively, old cells may simply lose their ability to sense nutrient availability and/or to uptake nutrients, resulting in the activation of CR pathways.

Old cells show distinct aging signatures

The aging proteome showed functional features that are consistent with many previous observations of changes in old cells. First, mitochondria function and integrity is weakened and disrupted in old cells due to accumulation of oxidative damage [66]. In the aging proteome, significantly reduced protein levels were observed for mitochondria components and metabolic enzymes. Second, cell wall components are increased in the aging proteome, consistent with cell wall expansion with age. Third, telomere chromatin structure is compromised and derepressed in old cells [1, 67], and we found significant increase in the aging proteome of the level of helicases encoded by telomere Y' elements.

The aging proteome also unveiled numerous novel features. One striking alteration is downregulation of ribosome abundance and protein translation. Ribosome biogenesis is elaborately controlled in eukaryotic cells, requiring coordinate regulation of all RNA polymerases. Hence, ribosome abundance is closely linked to the cellular metabolic state (Lempiäinen and Shore, 2009). CR extends lifespan by inhibiting ribosome biogenesis through the conserved TOR signaling pathway [34]. Although protein biosynthesis is greatly reduced in old cells, the underlying mechanism was unclear [42]. Our aging proteomic analysis showed for the first time the age-associated decline of ribosome abundance in old cells cultured in rich media. Notably, this decline is not caused by nutrient limitation, but rather results from an unknown mechanism in old cells. We showed by statistical tests that several categories of differentially regulated proteins in old cells resemble changes found in calorie-restricted young cells, including reduced ribosome abundance and elevated stress responses. Hence, we hypothesize that old cells exploit mechanisms activated by CR to antagonize aging and promote survival.

The aging proteome under CR reveals more aging-specific changes

Yeast cells cultured in various CR conditions show reduced levels of oxidative damage and extended lifespan. A number of factors and pathways have been attributed to the lifespan extension effect of CR, such as downregulated ribosome abundance through reduced TOR signaling, increased respiration and oxidative stress resistance, improved DNA damage response, and activation of Sir2. Nevertheless, cells still have limited lifespan under such conditions. Given our finding that old cells cultured in rich media show CR features, it becomes interesting to examine cells aged under CR conditions. Our proteomic analysis represents the first examination of age-associated proteomic changes in cells cultured and aged in CR media. While several features still underlie the anti-aging character of CR, such as further increased stress response and elevated amino acid biosynthesis, there is the clear omission of further reduction of ribosome levels. Importantly, other features revealed in the aging proteome in CR likely represent those changes detrimental to cell survival, such as the reduction of cellular membrane, mitochondria, and Ty1 reproduction — these may be invariant properties of aging cells that may not be altered by CR.

The aging proteome analysis is an approach for aging factor screen

A comprehensive analysis of yeast aging proteome provides the most straightforward information for what happened to the cell during aging. The

top-changed proteins during aging are the ones that react mostly to the aging mechanism. Analyzing these proteins by GO categories and how they change under NR and CR condition, we can learn more about the potential causing factors of aging. From the lifespan analysis, all the downregulated proteins showed reduced lifespan when deleted, corresponding to our prediction that these proteins are beneficial for cellular health and survival, as they fall into DNA replication and unfolded protein response category. If a protein is accumulating with time, it either drives the system into aging state or serve as an indicator of cellular stress. The proteins that are upregulated either only in NR condition or in both NR and CR condition fall into similar GO categories: cytoplasmic and vacuolar protein quality control regulation. They also show similar mixed results of lifespan when deleted. Loss of proteostasis is a hallmark of aging [48]. Our results show that in yeast, proteostasis is a major player in aging regulation.

Mitochondrial cholesterol control is a potential new aging pathway

From this study, we took Npc2 as an example to show that this screen can give us new targets of aging mechanisms. As a widely studied pathologic protein in neurodegenerative diseases, the *NPC2*-mitochondrial pathway can open a door to further aging and pathological research. The NPC1/NPC2 protein levels in aged mammalian kidney tissues and fibroblasts are significantly downregulated [68]. NPC1/NPC2 deficiency causes accumulation of unesterified cholesterol in the lysosome, leading to lysosomal disorder and neurodegeneration [69]. In yeast, deletion of either *NPC2* or *NCR1* will failure of sterol transportation from lipid droplets to vacuolar membrane [55]. It is reported that NPC2-knockdown will also cause decreased mitochondrial respiration function in liver fibroblasts [70] and adipocytes [71], supporting the idea that mitochondria are a downstream target regulated by NPC2. NPC2 transfers cholesterol directly from endosome to mitochondria in Chinese hamster ovary cells [72]. We observed decreased mitochondrial gene expression related to oxidative phosphorylation and respiration, reflected by decreased mtDNA and ATP production in *NPC2*-deficient cells. Combined with the fact that these cells survive better on non-fermentable carbon source, we speculate that deletion of *NPC2* causes alteration in mitochondria function, thereby creating a shift toward glycolysis instead of OXPHOS. There is data supporting increased glycolysis in mammalian *NPC1*-deficient cells [73], but the metabolic condition in *NPC2*-deficient cells, and detailed mechanisms leading to extended lifespan remains to be determined. The change in mitochondrial cholesterol leading to glycolysis metabolic shift that benefits longevity could be a novel aging pathway that has implications in human disease treatment.

Npc2 is increased in aging yeast. Here we reported several phenotypes of *npc2Δ* cells, including reduced mitochondrial gene expression, reduced ATP production and potential enhanced glycolysis activity. In our study, double deletion of *ERG6* and *NPC2* causes significant shortened lifespan (Fig. 4c), implicating that the balance of intracellular ergosterol is necessary to maintain cellular survival. Although 80% of yeast ergosterol is located at cytoplasmic membrane [74], mitochondrial ergosterol has been shown to play important roles in stress response [75]. On the other hand, biosynthesis of ergosterol is critical for mitochondrial morphogenesis [76]. One study showed that the alteration of the ergosterol distribution of mitochondria and ER membrane is sufficient to determine the efficiency of the insertion of tail-anchored proteins into mitochondrial outer membranes [77]. The unknown link between Npc2 and mitochondrial respiratory function can be related to these factors: mitochondrial ergosterol distribution, mitochondrial membrane proteins, and mitochondrial stress response.

In mammalian cells, NPC1 works with NPC2 as a tag team duo to transport cholesterol out of lysosomes [78]. The Niemann-Pick type C (NPC) disease is caused by mutations in either the NPC1 (95%) or NPC2 (5%) genes [52]. *NCR1* is the homolog of NPC1 in yeast. The deletion *NCR1* also significantly extends yeast lifespan (Fig. 4b). However, whether the *NCR1*-meditated longevity pathway shares similar mechanisms with *NPC2*-meditated longevity pathway remains to be explored. Ncr1 is responsible for subcellular sphingolipid distribution [54] and deletion of *NCR1* also shows mitochondrial dysfunctions [79]. It has been shown that this sphingolipid signaling pathway regulates downstream Pkh1p-Sch9p axis and thus mediates mitochondrial dysfunction and oxidative

stress sensitivity [79]. Whether this pathway is also responsible for *NCR1*-mediated replicative lifespan extension remains to be determined. Yeast cells experience a shift from fermentation to respiration during replicative aging [80]. Moreover, inhibiting mitochondrial respiration apparatus activates stress response and antagonizes aging [81]. Hence, we propose that metabolic interventions causing a shift from respiration toward glycolysis, as it occurs in *npc2Δ* cells, promote longevity.

Acknowledgements We would like to thank Dr. Shelley Berger (UPenn) for her advice on this project. We also thank Dr. Michiel Vermeulen and Pascal Jansen (The Radboud University Medical Centre) for providing mass spectrometry analysis service.

Author contribution Conceptualization, YS and WD; data curation, YS, RY, and WD; formal analysis, YS, RY, HG, HQ, and WD; funding acquisition, HQ, and WD; investigation, YS, RY, and HG; methodology, YS, RY, HG, and WD; project administration, YS and WD; resources, HQ, and WD; supervision, WD; validation, YS, RY and WD; writing — original draft, YS, RY and WD; writing — review and editing, YS, RY, HQ, and WD.

Funding This study was supported by NIH grants K99/R00AG037646, R56AG049714, R01AG052507, and R41/R42AG058368 to WD, CPRIT Scholar award R1306 to WD, Welch Foundation grant Q-1986–20190330 to WD, NSF award #1720215, #1761839, and internal support of the University of Tennessee at Chattanooga to HQ.

Availability of data and material The mass spectrometry proteomics data have been deposited to the ProteomeXchange Consortium via the PRIDE partner repository with the dataset identifier PXD018917. The RNA-seq data have been deposited to SRA under accession number PRJNA715646.

All experimental materials generated by this study are available upon request.

Code availability Not applicable.

Declarations

Competing interests The authors declare no competing interests.

Ethics approval Not applicable.

Consent to participate Not applicable.

Consent for publication All authors have agreed to the content of this manuscript for publication.

References

1. Dang W, Steffen KK, Perry R, Dorsey JA, Johnson FB, Shilatifard A, et al. Histone H4 lysine 16 acetylation regulates cellular lifespan. Nature. 2009;459(7248):802–7. https://doi.org/10.1038/nature08085.
2. Kirmizis A, Santos-Rosa H, Penkett CJ, Singer MA, Vermeulen M, Mann M, et al. Arginine methylation at histone H3R2 controls deposition of H3K4 trimethylation. Nature. 2007;449(7164):928–32. https://doi.org/10.1038/nature06160.
3. Rappsilber J, Mann M. Analysis of the topology of protein complexes using cross-linking and mass spectrometry. CSH Protoc. 2007;2007:pdb prot4594. doi:https://doi.org/10.1101/pdb.prot4594.
4. Cox J, Mann M (2008) MaxQuant enables high peptide identification rates, individualized p.p.b.-range mass accuracies and proteome-wide protein quantification. Nat Biotechnol 26(12):1367–72. doi:https://doi.org/10.1038/nbt.1511.
5. Cox J, Neuhauser N, Michalski A, Scheltema RA, Olsen JV, Mann M. Andromeda: a peptide search engine integrated into the MaxQuant environment. J Proteome Res. 2011;10(4):1794–805. https://doi.org/10.1021/pr101065j.
6. da Huang W, Sherman BT, Lempicki RA. Systematic and integrative analysis of large gene lists using DAVID bioinformatics resources. Nat Protoc. 2009;4(1):44–57. https://doi.org/10.1038/nprot.2008.211.
7. Huang da W, Sherman BT, Zheng X, Yang J, Imamichi T, Stephens R et al. (2009) Extracting biological meaning from large gene lists with DAVID. Curr Protoc Bioinformatics, Chapter 13:Unit 13 1. doi:https://doi.org/10.1002/0471250953.bi1311s27.
8. Oughtred R, Stark C, Breitkreutz B-J, Rust J, Boucher L, Chang C, et al. The BioGRID interaction database: 2019 update. Nucleic Acids Res. 2019;47(D1):D529–41. https://doi.org/10.1093/nar/gky1079.
9. Maslov S, Sneppen K. Specificity and stability in topology of protein networks. Science. 2002;296(5569):910–3.
10. Jo MC, Liu W, Gu L, Dang W, Qin L. High-throughput analysis of yeast replicative aging using a microfluidic system. Proc Natl Acad Sci U S A. 2015;112(30):9364–9. https://doi.org/10.1073/pnas.1510328112.
11. Guarente L. Mitochondria–a nexus for aging, calorie restriction, and sirtuins? Cell. 2008;132(2):171–6. https://doi.org/10.1016/j.cell.2008.01.007.
12. Feser J, Tyler J. Chromatin structure as a mediator of aging. FEBS Lett. 2011;585(13):2041–8. https://doi.org/10.1016/j.febslet.2010.11.016.
13. Sahin E, Depinho RA. Linking functional decline of telomeres, mitochondria and stem cells during ageing. Nature. 2010;464(7288):520–8. https://doi.org/10.1038/nature08982.
14. Kourtis N, Tavernarakis N. Cellular stress response pathways and ageing: intricate molecular relationships. EMBO J. 2011;30(13):2520–31. https://doi.org/10.1038/emboj.2011.162.
15. Landis GN, Tower J. Superoxide dismutase evolution and life span regulation. Mech Ageing Dev. 2005;126(3):365–79. https://doi.org/10.1016/j.mad.2004.08.012.

16. Koga H, Kaushik S, Cuervo AM. Protein homeostasis and aging: the importance of exquisite quality control. Ageing Res Rev. 2011;10(2):205–15. https://doi.org/10.1016/j.arr.2010.02.001.
17. Green DR, Galluzzi L, Kroemer G. Mitochondria and the autophagy-inflammation-cell death axis in organismal aging. Science. 2011;333(6046):1109–12. https://doi.org/10.1126/science.1201940.
18. Mostoslavsky R, Chua KF, Lombard DB, Pang WW, Fischer MR, Gellon L, et al. Genomic instability and aging-like phenotype in the absence of mammalian SIRT6. Cell. 2006;124(2):315–29. https://doi.org/10.1016/j.cell.2005.11.044.
19. Gorbunova V, Seluanov A, Mao Z, Hine C. Changes in DNA repair during aging. Nucleic Acids Res. 2007;35(22):7466–74. https://doi.org/10.1093/nar/gkm756.
20. Lin SS, Manchester JK, Gordon JI. Enhanced gluconeogenesis and increased energy storage as hallmarks of aging in Saccharomyces cerevisiae. J Biol Chem. 2001;276(38):36000–7. https://doi.org/10.1074/jbc.M103509200.
21. Lund J, Tedesco P, Duke K, Wang J, Kim SK, Johnson TE. Transcriptional profile of aging in C. elegans. Curr Biol. 2002;12(18):1566–73.
22. Lesur I, Campbell JL. The transcriptome of prematurely aging yeast cells is similar to that of telomerase-deficient cells. Mol Biol Cell. 2004;15(3):1297–312. https://doi.org/10.1091/mbc.e03-10-0742.
23. Laun P, Ramachandran L, Jarolim S, Herker E, Liang P, Wang J, et al. A comparison of the aging and apoptotic transcriptome of Saccharomyces cerevisiae. FEMS Yeast Res. 2005;5(12):1261–72. https://doi.org/10.1016/j.femsyr.2005.07.006.
24. Zhan M, Yamaza H, Sun Y, Sinclair J, Li H, Zou S. Temporal and spatial transcriptional profiles of aging in Drosophila melanogaster. Genome Res. 2007;17(8):1236–43. https://doi.org/10.1101/gr.6216607.
25. de Godoy LM, Olsen JV, Cox J, Nielsen ML, Hubner NC, Frohlich F, et al. Comprehensive mass-spectrometry-based proteome quantification of haploid versus diploid yeast. Nature. 2008;455(7217):1251–4. https://doi.org/10.1038/nature07341.
26. Feser J, Truong D, Das C, Carson JJ, Kieft J, Harkness T, et al. Elevated histone expression promotes life span extension. Mol Cell. 2010;39(5):724–35. https://doi.org/10.1016/j.molcel.2010.08.015.
27. Xie F, Liu T, Qian WJ, Petyuk VA, Smith RD. Liquid chromatography-mass spectrometry-based quantitative proteomics. J Biol Chem. 2011;286(29):25443–9. https://doi.org/10.1074/jbc.R110.199703.
28. Cox J, Mann M. Quantitative, high-resolution proteomics for data-driven systems biology. Annu Rev Biochem. 2011;80:273–99. https://doi.org/10.1146/annurev-biochem-061308-093216.
29. Walther DM, Mann M (2011) Accurate quantification of more than 4000 mouse tissue proteins reveals minimal proteome changes during aging. Mol Cell Proteomics 10(2):M110 004523. doi:https://doi.org/10.1074/mcp.M110.004523.
30. Jazwinski SM. Yeast longevity and aging–the mitochondrial connection. Mech Ageing Dev. 2005;126(2):243–8. https://doi.org/10.1016/j.mad.2004.08.016.
31. Thorpe PH, Bruno J, Rothstein R. Modeling stem cell asymmetry in yeast. Cold Spring Harb Symp Quant Biol. 2008;73:81–8. https://doi.org/10.1101/sqb.2008.73.010.
32. Mair W, Dillin A. Aging and survival: the genetics of life span extension by dietary restriction. Annu Rev Biochem. 2008;77:727–54. https://doi.org/10.1146/annurev.biochem.77.061206.171059.
33. Kaeberlein M, Powers RW 3rd, Steffen KK, Westman EA, Hu D, Dang N, et al. Regulation of yeast replicative life span by TOR and Sch9 in response to nutrients. Science. 2005;310(5751):1193–6. https://doi.org/10.1126/science.1115535.
34. Steffen KK, MacKay VL, Kerr EO, Tsuchiya M, Hu D, Fox LA, et al. Yeast life span extension by depletion of 60s ribosomal subunits is mediated by Gcn4. Cell. 2008;133(2):292–302. https://doi.org/10.1016/j.cell.2008.02.037.
35. Vaquero A, Reinberg D. Calorie restriction and the exercise of chromatin. Genes Dev. 2009;23(16):1849–69. https://doi.org/10.1101/gad.1807009.
36. Lin SJ, Defossez PA, Guarente L. Requirement of NAD and SIR2 for life-span extension by calorie restriction in Saccharomyces cerevisiae. Science. 2000;289(5487):2126–8.
37. Lin SJ, Ford E, Haigis M, Liszt G, Guarente L. Calorie restriction extends yeast life span by lowering the level of NADH. Genes Dev. 2004;18(1):12–6. https://doi.org/10.1101/gad.1164804.
38. Lin SJ, Kaeberlein M, Andalis AA, Sturtz LA, Defossez PA, Culotta VC, et al. Calorie restriction extends Saccharomyces cerevisiae lifespan by increasing respiration. Nature. 2002;418(6895):344–8. https://doi.org/10.1038/nature00829.
39. Molin M, Yang J, Hanzen S, Toledano MB, Labarre J, Nystrom T. Life span extension and H(2)O(2) resistance elicited by caloric restriction require the peroxiredoxin Tsa1 in Saccharomyces cerevisiae. Mol Cell. 2011;43(5):823–33. https://doi.org/10.1016/j.molcel.2011.07.027.
40. Ristow M, Schmeisser S. Extending life span by increasing oxidative stress. Free Radic Biol Med. 2011;51(2):327–36. https://doi.org/10.1016/j.freeradbiomed.2011.05.010.
41. Vermeulen M, Eberl HC, Matarese F, Marks H, Denissov S, Butter F, et al. Quantitative interaction proteomics and genome-wide profiling of epigenetic histone marks and their readers. Cell. 2010;142(6):967–80. https://doi.org/10.1016/j.cell.2010.08.020.
42. Rattan SI. Synthesis, modification and turnover of proteins during aging. Adv Exp Med Biol. 2010;694:1–13.
43. Powell CD, Quain DE, Smart KA. The impact of brewing yeast cell age on fermentation performance, attenuation and flocculation. FEMS Yeast Res. 2003;3(2):149–57. https://doi.org/10.1016/S1567-1356(03)00002-3.
44. Erjavec N, Larsson L, Grantham J, Nystrom T. Accelerated aging and failure to segregate damaged proteins in Sir2 mutants can be suppressed by overproducing the protein aggregation-remodeling factor Hsp104p. Genes

Dev. 2007;21(19):2410–21. https://doi.org/10.1101/gad.439307.
45. Orlandi I, Bettiga M, Alberghina L, Nystrom T, Vai M. Sir2-dependent asymmetric segregation of damaged proteins in ubp10 null mutants is independent of genomic silencing. Biochim Biophys Acta. 2010;1803(5):630–8. https://doi.org/10.1016/j.bbamcr.2010.02.009.
46. Kaeberlein M. Lessons on longevity from budding yeast. Nature. 2010;464(7288):513–9. https://doi.org/10.1038/nature08981.
47. Friis RM, Wu BP, Reinke SN, Hockman DJ, Sykes BD, Schultz MC. A glycolytic burst drives glucose induction of global histone acetylation by picNuA4 and SAGA. Nucleic Acids Res. 2009;37(12):3969–80. https://doi.org/10.1093/nar/gkp270.
48. Lopez-Otin C, Blasco MA, Partridge L, Serrano M, Kroemer G. The hallmarks of aging. Cell. 2013;153(6):1194–217. https://doi.org/10.1016/j.cell.2013.05.039.
49. Kaushik S, Cuervo AM. Proteostasis and aging. Nat Med. 2015;21(12):1406–15. https://doi.org/10.1038/nm.4001.
50. Janssens GE, Meinema AC, Gonzalez J, Wolters JC, Schmidt A, Guryev V, et al. Protein biogenesis machinery is a driver of replicative aging in yeast. Elife. 2015;4:e08527. https://doi.org/10.7554/eLife.08527.
51. Berger AC, Vanderford TH, Gernert KM, Nichols JW, Faundez V, Corbett AH. Saccharomyces cerevisiae Npc2p is a functionally conserved homologue of the human Niemann-Pick disease type C 2 protein, hNPC2. Eukaryot Cell. 2005;4(11):1851–62. https://doi.org/10.1128/EC.4.11.1851-1862.2005.
52. Newton J, Milstien S, Spiegel S. Niemann-Pick type C disease: The atypical sphingolipidosis. Adv Biol Regul. 2018;70:82–8. https://doi.org/10.1016/j.jbior.2018.08.001.
53. Zhang S, Ren J, Li H, Zhang Q, Armstrong JS, Munn AL, et al. Ncr1p, the yeast ortholog of mammalian Niemann Pick C1 protein, is dispensable for endocytic transport. Traffic. 2004;5(12):1017–30. https://doi.org/10.1111/j.1600-0854.2004.00241.x.
54. Malathi K, Higaki K, Tinkelenberg AH, Balderes DA, Almanzar-Paramio D, Wilcox LJ, et al. Mutagenesis of the putative sterol-sensing domain of yeast Niemann Pick C-related protein reveals a primordial role in subcellular sphingolipid distribution. J Cell Biol. 2004;164(4):547–56. https://doi.org/10.1083/jcb.200310046.
55. Winkler MBL, Kidmose RT, Szomek M, Thaysen K, Rawson S, Muench SP, et al. Structural insight into eukaryotic sterol transport through Niemann-Pick type C proteins. Cell. 2019. https://doi.org/10.1016/j.cell.2019.08.038.
56. Hu Z, He B, Ma L, Sun Y, Niu Y, Zeng B. Recent advances in ergosterol biosynthesis and regulation mechanisms in Saccharomyces cerevisiae. Indian J Microbiol. 2017;57(3):270–7. https://doi.org/10.1007/s12088-017-0657-1.
57. Vambutas A, Ackerman SH, Tzagoloff A. Mitochondrial translational-initiation and elongation factors in Saccharomyces cerevisiae. Eur J Biochem. 1991;201(3):643–52.
58. Ott M, Amunts A, Brown A. Organization and regulation of mitochondrial protein synthesis. Annu Rev Biochem. 2016;85:77–101. https://doi.org/10.1146/annurev-biochem-060815-014334.
59. Medvedik O, Lamming DW, Kim KD, Sinclair DA. MSN2 and MSN4 link calorie restriction and TOR to sirtuin-mediated lifespan extension in Saccharomyces cerevisiae. PLoS Biol. 2007;5(10): e261. https://doi.org/10.1371/journal.pbio.0050261.
60. Beach A, Leonov A, Arlia-Ciommo A, Svistkova V, Lutchman V, Titorenko VI. Mechanisms by which different functional states of mitochondria define yeast longevity. Int J Mol Sci. 2015;16(3):5528–54. https://doi.org/10.3390/ijms16035528.
61. Guaragnella N, Coyne LP, Chen XJ, Giannattasio S. (2018) Mitochondria-cytosol-nucleus crosstalk: learning from Saccharomyces cerevisiae. FEMS Yeast Res 18(8). doi:https://doi.org/10.1093/femsyr/foy088
62. Liu Z, Butow RA. Mitochondrial retrograde signaling. Annu Rev Genet. 2006;40:159–85. https://doi.org/10.1146/annurev.genet.40.110405.090613.
63. Zorova LD, Popkov VA, Plotnikov EY, Silachev DN, Pevzner IB, Jankauskas SS, et al. Mitochondrial membrane potential. Anal Biochem. 2018;552:50–9. https://doi.org/10.1016/j.ab.2017.07.009.
64. Jury DR, Kaveti S, Duan ZH, Willard B, Kinter M, Londraville R. Effects of calorie restriction on the zebrafish liver proteome. Comp Biochem Physiol Part D Genomics Proteomics. 2008;3(4):275–82. https://doi.org/10.1016/j.cbd.2008.07.003.
65. Valle A, Sastre-Serra J, Roca P, Oliver J. Modulation of white adipose tissue proteome by aging and calorie restriction. Aging Cell. 2010;9(5):882–94. https://doi.org/10.1111/j.1474-9726.2010.00613.x.
66. Steinkraus KA, Kaeberlein M, Kennedy BK. Replicative aging in yeast: the means to the end. Annu Rev Cell Dev Biol. 2008;24:29–54. https://doi.org/10.1146/annurev.cellbio.23.090506.123509.
67. Kim S, Villeponteau B, Jazwinski SM. Effect of replicative age on transcriptional silencing near telomeres in Saccharomyces cerevisiae. Biochem Biophys Res Commun. 1996;219(2):370–6. https://doi.org/10.1006/bbrc.1996.0240.
68. Konig J, Besoke F, Stuetz W, Malarski A, Jahreis G, Grune T, et al. Quantification of age-related changes of alpha-tocopherol in lysosomal membranes in murine tissues and human fibroblasts. BioFactors. 2016;42(3):307–15. https://doi.org/10.1002/biof.1274.
69. Demais V, Barthelemy A, Perraut M, Ungerer N, Keime C, Reibel S, et al. Reversal of pathologic lipid accumulation in NPC1-deficient neurons by drug-promoted release of LAMP1-coated lamellar inclusions. J Neurosci. 2016;36(30):8012–25. https://doi.org/10.1523/JNEUROSCI.0900-16.2016.
70. Wang YH, Twu YC, Wang CK, Lin FZ, Lee CY, Liao YJ. (2018) Niemann-Pick type C2 protein regulates free cholesterol accumulation and influences hepatic stellate cell proliferation and mitochondrial respiration function. Int J Mol Sci 19(6). doi:https://doi.org/10.3390/ijms19061678
71. Guo H, Zhao M, Qiu X, Deis JA, Huang H, Tang QQ, et al. Niemann-Pick type C2 deficiency impairs autophagy-lysosomal activity, mitochondrial function, and TLR signaling in adipocytes. J Lipid Res. 2016;57(9):1644–58. https://doi.org/10.1194/jlr.M066522.

72. Kennedy BE, Charman M, Karten B. Niemann-Pick Type C2 protein contributes to the transport of endosomal cholesterol to mitochondria without interacting with NPC1. J Lipid Res. 2012;53(12):2632–42. https://doi.org/10.1194/jlr.M029942.
73. Kennedy BE, Madreiter CT, Vishnu N, Malli R, Graier WF, Karten B. Adaptations of energy metabolism associated with increased levels of mitochondrial cholesterol in Niemann-Pick type C1-deficient cells. J Biol Chem. 2014;289(23):16278–89. https://doi.org/10.1074/jbc.M114.559914.
74. Solanko LM, Sullivan DP, Sere YY, Szomek M, Lunding A, Solanko KA, et al. Ergosterol is mainly located in the cytoplasmic leaflet of the yeast plasma membrane. Traffic. 2018;19(3):198–214. https://doi.org/10.1111/tra.12545.
75. Nielson JR, Fredrickson EK, Waller TC, Rendon OZ, Schubert HL, Lin Z et al. (2017) Sterol oxidation mediates stress-responsive Vms1 translocation to mitochondria. Mol Cell 68(4):673–85 e6. doi:https://doi.org/10.1016/j.molcel.2017.10.022
76. Altmann K, Westermann B. Role of essential genes in mitochondrial morphogenesis in Saccharomyces cerevisiae. Mol Biol Cell. 2005;16(11):5410–7. https://doi.org/10.1091/mbc.e05-07-0678.
77. Krumpe K, Frumkin I, Herzig Y, Rimon N, Ozbalci C, Brugger B, et al. Ergosterol content specifies targeting of tail-anchored proteins to mitochondrial outer membranes. Mol Biol Cell. 2012;23(20):3927–35. https://doi.org/10.1091/mbc.E11-12-0994.
78. Infante RE, Wang ML, Radhakrishnan A, Kwon HJ, Brown MS, Goldstein JL. NPC2 facilitates bidirectional transfer of cholesterol between NPC1 and lipid bilayers, a step in cholesterol egress from lysosomes. Proc Natl Acad Sci U S A. 2008;105(40):15287–92. https://doi.org/10.1073/pnas.0807328105.
79. Vilaca R, Silva E, Nadais A, Teixeira V, Matmati N, Gaifem J, et al. Sphingolipid signalling mediates mitochondrial dysfunctions and reduced chronological lifespan in the yeast model of Niemann-Pick type C1. Mol Microbiol. 2014;91(3):438–51. https://doi.org/10.1111/mmi.12470.
80. Leupold S, Hubmann G, Litsios A, Meinema AC, Takhaveev V, Papagiannakis A et al. (2019) Saccharomyces cerevisiae goes through distinct metabolic phases during its replicative lifespan. Elife 8. doi:https://doi.org/10.7554/eLife.41046
81. Peric M, Bou Dib P, Dennerlein S, Musa M, Rudan M, Lovric A, et al. Crosstalk between cellular compartments protects against proteotoxicity and extends lifespan. Sci Rep. 2016;6:28751. https://doi.org/10.1038/srep28751.